Available online at www.sciencedirect.com

ScienceDirect

IFAC Papers Online CONFERENCE PAPER ARCHIVE

IFAC PapersOnLine 50-1 (2017) 10052–10057

A Novel Energy Management Strategy for Fuel-Cell/Supercapacitor Hybrid Vehicles ⋆

M. Carignano * **R. Costa-Castelló** ** **N. Nigro** *** **S. Junco** ****

* *Escuela de Ingeniería Mecánica, Universidad Nacional de Rosario, UNR-CONICET, Rosario, Argentina, (e-mail: mauroc@fceia.unr.edu.ar).*

** *Universitat Politècnica de Catalunya, Barcelona, Spain, (e-mail: ramon.costa@upc.edu).*

*** *Centro de Investigación de Métodos Computacionales, CIMEC-CONICET-UNL, Santa Fe, Argentina, (e-mail: norberto.nigro@cimec.santafe-conicet.gov.ar).*

**** *Departamento de Control, Universidad Nacional de Rosario, Rosario, Argentina, (e-mail: sjunco@fceia.unr.edu.ar).*

Abstract: Hybrid platforms powered by fuel cell and supercapacitor represent a powertrain with active state-dependent constraints, providing an adverse scenario for the energy management. In these platforms, the performance of the vehicle in terms of efficiency and power compliance is noticeably affected by the energy management strategy. This paper presents a novel energy management strategy based on the estimation of the future energy demand. The strategy aims for maintaining the state of energy of the supercapacitor between two limits, which are computed online using the states of the system. The performance of the proposed strategy is tested by simulation in a hybrid electric bus operated under real urban driving conditions. The results show improvements on hydrogen consumption and on power compliance compared to the widely reported Equivalent Consumption Minimization Strategy. Also, the results include the comparison with the optimal strategy obtained offline through Dynamic Programming.

Keywords: Hybrid Vehicle, Fuel Cell, Supercapacitor, Constraints, Energy Management.

1. INTRODUCTION

Fuel Cell Hybrid Vehicles (FCHV) represent a solution of increasing interest for car manufactures. Nevertheless, some matters associated to hydrogen (H_2) production, distribution and storage; and fuel cell cost and lifetime, must be improved to make this technology more profitable and affordable. A complete description of issues and challenges on FCHV is presented by Sulaiman et al. (2015), while the current status of HEV and comparisons between the different technologies is addressed by Pollet et al. (2012). The Fuel Cell (FC) offers two main advantages compared to the internal combustion engines: higher efficiency and zero emissions. However, despite these advantages, the FC presents some limitations associated with its slow transient response. The reported literature points out that fast power variations promote the damage of the FC (Strahl et al. (2014); Borup et al. (2007)). To avoid that, the power rates of the FC is usually bounded, and to fulfill such highly variant power profiles, FCHVs incorporate an energy storage system. Additionally, this energy storage system allows to recover energy from braking. Generally, a battery and/or a SC is adopted.

From the point of view of the energy management strategy (EMS), FCHVs with SC represent and adverse scenario due to the presence of active state-dependent constraints. Such constraints affect sensitively both the H_2 consumption and the fulfillment of power demand. A review of EMS for FCHV presented by Sulaiman et al. (2015) points out that the Equivalent Consumption Minimization Strategy (ECMS) is the most outstanding strategy. Rodatz et al. (2005) present a complete description of the ECMS and the implementation, including experimental validation, in a FCHV with SC. Although ECMS provides a close-to-optimal solution in a wide range of hybrid platforms, the differences with the optimal solution increases in case of system with active state-dependent constrains. A comparison presented by Feroldi and Carignano (2016) shows differences higher than 10% between the ECMS and the optimal offline strategy. In contrast to optimization approaches, heuristic strategies based on rules are reported in the literature (Feroldi et al. (2009)). This approach offers in general an acceptable performance and lower computing time, which become more suitable for real time applications.

In this work, a new EMS for a FCHV with SC based on energy estimations is presented. The strategy is specially designed for cases where the state-dependent constraints of system are often active in operation.

⋆ This work has been supported by the scholarship program BECAR of Ministerio de Modernización of Argentina, by the project DPI2015-69286-C3-2-R (MINECO/FEDER) and by the European Commission H2020 under the Fuel Cell and Hydrogen Joint Undertaking project INN-BALANCE #735969.

10.1016/j.ifacol.2017.08.1776

2. VEHICLE MODEL

The configuration of the FCHV adopted in this work is shown in Fig. 1. The power at wheels is provided by the Electric Machine (EM). The EM can also work as generator to recover energy from braking, and it is connected to direct current bus (DC-BUS) through a bidirectional Converter. Then, the FC delivers power through the Boost converter to the DC-BUS, while the SC delivers or receives power through the Buck/Boost converter. The model of the powertrain used to evaluate the H_2 consumption and the power compliance is focused on the efficiency and on the constraints, neglecting its dynamics. The electronic converters Buck/Boost and Boost are included in the model through their efficiencies, η_{BB} and η_{BO}, and through their maximum power P_{BB}^{max} and P_{BO}^{max} respectively. In both cases, the maximum power are referred on the DC-BUS side. In case of Buck/Boost, due to the high variation of voltage of SC, the current on the SC side is limited. Alternatively, the Differential is included in the model through its transmission ratio i_{DF} and its efficiency η_{DF}. Finally, for the EM, the maximum torque T_{EM}^{max}, the maximum mechanical power P_{EM}^{max} and its efficiency η_{EM} (which includes that of Converter) are considered.

2.1 Fuel cell model

For the purposes of this work, the FC is reduced to a first order model, including its efficiency and constraints. The H_2 consumption is computed from a map, and in this case a FC of 50KW from the software ADVISOR is used. It is valuable to notice that this map take into account the power required for the auxiliary components. Concerning its dynamics, the instantaneous FC power is considered as a state variable, and its discrete-time state equation is:

$$x_{FC}(k+1) = x_{FC}(k) + \Delta P_{FC}(k)\ t_s, \tag{1}$$

where ΔP_{FC} is the gradient of power and t_s the sampling time. Then, assuming the variation of power on FC follows a ramp form, the average power delivered in an interval results:

$$P_{FC}(k) = x_{FC}(k) + 0.5\ \Delta P_{FC}(k)\ t_s. \tag{2}$$

Regarding the constraints, the power state is bounded: $0 \leq x_{FC}(k) \leq P_{FC}^{max}$; and also a maximum power rate is allowed. The latter imposes hard constraints for the EMS, affecting noticeably the vehicle performance. Currently, it is not entirely clear how to establish accurately the power rate limits to assure non-premature aging of FC. In general, fixed and conservative values are adopted. According to the reported literature, in this work a maximum 10% of the maximum power of the FC per second for rise and fall is assumed (Rodatz et al. (2005); Feroldi and Carignano (2016); Motapon et al. (2014)).

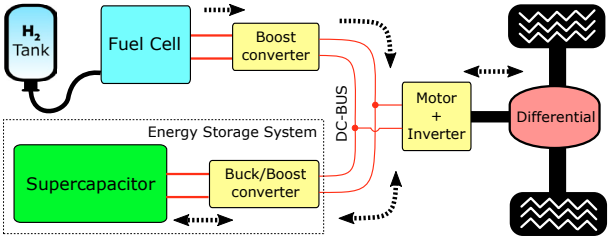

Fig. 1. FCHV configuration

2.2 Supercapacitor model

An analytic expression to model the SC can be deduced from the equivalent circuit composed by a capacitor and a resistor connected in series circuit (Guzzella et al. (2007)). The output voltage and the open-circuit voltage are:

$$U_{SC}(k) = U_{SC,oc}(k) - R_{SC} I_{SC}(k);\quad U_{SC,oc}(k) = \frac{Q_{SC}(k)}{C_{SC}}, \tag{3}$$

where R_{SC} is the internal resistance and C_{SC} is the capacity. The energy stored and the nominal energy of the SC can be written as follows:

$$E_{SC}(k) = 0.5\ C_{SC}\ U_{SC,oc}^2(k);\quad E_{SC,0} = 0.5\ C_{SC}\ U_{SC,0}^2, \tag{4}$$

where $U_{SC,0}$ is the nominal (or maximum) voltage. Then, the dynamics of the state of energy (SOE) can be expressed as follows,

$$SOE(k+1) = SOE(k) - \frac{U_{SC,oc}(k)\ I_{SC}(k)\ t_s}{E_{SC,0}}. \tag{5}$$

Note that the current in the SC is considered negative for charging. Concerning the constraint, fixed lower and upper limits are considered, i.e. $SOE_{min} \leq SOE(k) \leq SOE_{max}$.

2.3 Power required from DC-BUS

The torque required at the wheels is computed through a first order non-linear vehicle model that considers inertial forces, rolling resistance and aerodynamic drag. From the current speed of vehicle $v(k)$ and with the speed required at next step $v(k+1)$, the torque necessary at the wheels (T_{wh}) is computed using the following set of equations:

$$\begin{aligned} v_{avg}(k) &= 0.5\ (v(k) + v(k+1)) \\ F_{aero}(k) &= 0.5\ A_f\ C_x\ \rho_{air}\ v_{avg}^2(k) \\ F_{roll}(k) &= m\ 9.81\ (r_0 + r_1\ v_{avg}(k)) \\ F_{iner}(k) &= m\ a(k);\quad a(k) = t_s^{-1}(v(k+1) - v(k)) \\ T_{wh}(k) &= (F_{aero}(k) + F_{roll}(k) + F_{iner}(k))\ R_{wh}, \end{aligned} \tag{6}$$

where v_{avg} and a are the average speed and acceleration in the time interval respectively; m is the total mass of the vehicle; A_f, C_x and ρ are frontal area, drag coefficient and air density respectively; r_0 and r_1 are rolling resistance coefficients; and R_{wh} is the wheel radius. Then, the speed and torque required to the EM results;

$$\omega_{EM}(k) = \frac{v_{avg}(k)\ i_{DF}}{R_{wh}};\quad T_{EM}^{req}(k) = \frac{T_{wh}(k)}{i_{DF}}\ \eta_{DF}^{-sign(T_{wh}(k))}. \tag{7}$$

When the EM is not able to produce the negative torque required for braking, therefore its maximum negative torque available is used, and, to fulfill the demand, the dissipative brake is employed. On the contrary, when the EM is not able to produce the positive torque required for propulsion, therefore its maximum available torque is used, and in this case the speed required is not achieved. Then, the power required by the Converter to DC-BUS results:

$$P_{CON}^{req}(k) = T_{EM}(k)\ \omega_{EM}(k)\ \eta_{EM}^{-sign(T_{EM}(k))}. \tag{8}$$

Notice that the power flow in the Converter is considered positive when the EM works as motor (propulsion).

2.4 Power required from the power sources

The power balance on the DC-BUS is:

$$P_{CON}(k) - P_{BO}(k) - P_{ESS}(k) = 0, \tag{9}$$

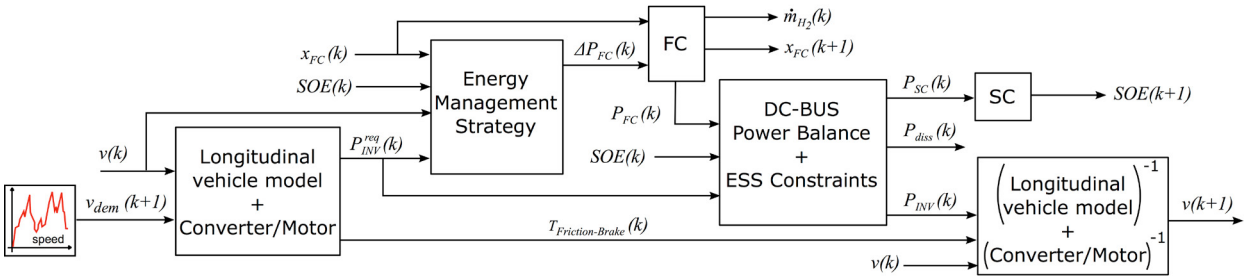

Fig. 2. Schematic representation of the model used to performs the simulations

where P_{CON}, P_{BO} and P_{ESS} are the power flow through Converter, Boost converter and Energy Storage System (ESS) respectively. According to this equation, and knowing that $P_{CON}(k)$ is determined by the driver, the propulsion system has a degree of freedom. In this case ΔP_{FC} was selected as control input. Once ΔP_{FC} is defined by the EMS, the power delivered by the FC is obtained by using Eq. (2), and the power delivered by the Boost converter results in,

$$P_{BO}(k) = P_{FC}(k)\ \eta_{BO}. \tag{10}$$

Then, from power demanded by the Converter, the power required from ESS can be obtained from Eq. (9) as follows:

$$P_{ESS}^{req}(k) = P_{CON}(k) - P_{BO}(k). \tag{11}$$

Now, the constraints associated to the ESS must be considered. They are the maximum/minimum power in Buck/Boost converter; the maximum/minimum current in the SC; and the maximum/minimum SOE. Accordingly, from the current SOE in SC, the maximum and minimum power available from ESS can be computed, namely P_{ESS}^{max} and P_{ESS}^{min}. Then, the power flow in Buck/Boost results in:

$$P_{BB}(k) = \max\left\{\min\left\{P_{ESS}^{req}(k); P_{ESS}^{max}(k)\right\}; P_{ESS}^{min}(k)\right\}. \tag{12}$$

In case of $P_{ESS}^{req}(k) < P_{ESS}^{min}$, a portion of power from DC-BUS can not be stored and must be dissipated:

$$P_{diss}(k) = P_{BB}(k) - P_{ESS,req}(k), \tag{13}$$

and otherwise, P_{diss} is equal zero. Particularly in case of $P_{ESS}^{req}(k) > P_{ESS}^{max}$, the power available from ESS is lower that the power required, therefore the speed demanded $v(k+1)$ will not be fulfilled. The new future speed, i.e. the speed attained in $k+1$, can be computed shifting the causality of equations presented. Finally, the power in the SC results,

$$P_{SC}(k) = P_{BB}(k)\eta_{BB}^{-sign(P_{BB}(k))}. \tag{14}$$

Fig. 2 shows a schematic representation of the causal model used to perform the simulations.

3. ENERGY-BASED ESTIMATION STRATEGY

The strategy proposed in this work, named hereafter Energy-based Estimation Strategy (EBES), has three goals: first, to provide at any time the power required to propel the vehicle; second, to recover as much energy as possible from braking; and finally to operate the FC at maximum efficiency. As it was mentioned, the input control variable of the propulsion system is ΔP_{FC}. In the first step, two supercapacitor SOE limits are computed, which are used then to define the fuel cell power reference. The procedure to compute such limits is described in the sequel.

3.1 Determination of the supercapacitor SOE limits

This step is the core of the strategy. Here, an upper and a lower limit of SOE are found. In contrast to previous published strategies (for example in Feroldi et al. (2009)), the limits of SOE are not fixed, but they are adapted in run time according to the vehicle speed and FC power state. Specifically, they are computed so that if the current SOE of SC is between them, the propulsion system is able to accelerate from the current speed up to a predefined maximum speed; and also, store overall energy produced by both the regenerative braking and FC from the current speed until it stops.

Trip energy estimation

An estimation of the energy required during a trip from v_0 to v_f may be estimated considering the variation of kinetic energy. However, such approximation neglects the dissipation effects produced by aerodynamics and rolling resistances. A more accurate estimation is obtained taking into account such effects. Then, the total energy required (at the wheels) is the sum of the three terms,

$$E_{trip} = E_{kin} + E_{aero} + E_{roll}, \tag{15}$$

where E_{kin}, E_{aero} and E_{roll} are the kinetic energy variation, the energy dissipated by aerodynamics effect and the energy dissipated by rolling resistance respectively. They can be computed easily from 6 easily assuming a constant acceleration a. Notice that the last two terms are always positive, while the first one depend on whether it is propulsion trip (positive) or braking trip (negative). Therefore, E_{trip} can be positive or negative.

Lower state of energy

The lower state of energy, namely SOE_{low}, is computed so that if the current SOE is higher than SOE_{low}, the propulsion system is able to provide the energy required to go from the current speed $v(k)$ up to a maximum predefined speed v_{max}. During a propulsion trip, the energy required from DC-BUS is computed using Eq.(15) with $v_0 = v(k)$ and $v_f = v_{max}$, and that using the component efficiencies, it is:

$$E_{pr}(k) = \frac{E_{trip}(k)}{\eta_{DF}\ \eta_{EM}}. \tag{16}$$

Then, this energy drawn from the DC-BUS must be supplied by the FC and by the SC, which leads to:

$$E_{SC}(k)\ \eta_{SC}\ \eta_{BB} + E_{FC}^{pr}(k)\ \eta_{BO} \geq E_{pr}(k), \tag{17}$$

where E_{SC} is the energy available in the SC (computed from (4)), η_{SC} is the average efficiency of SC, and E_{FC}^{pr} is

the maximum energy that the FC is able to provide during this trip. The latter is computed assuming that, from its current state, the FC rises up to its maximum power as fast as possible. Now, returning to (17), solving for E_{SC} and by expressing E_{SC} in term of SOE, the condition proposed leads to:

$$SOE(k) \geq \left(\frac{E_{pr}(k) - E_{FC}^{pr}(k)\ \eta_{BO}}{\eta_{SC}\ \eta_{BB}\ E_{SC,0}} \right). \tag{18}$$

Notice that by fulfilling this expression, the propulsion system has enough energy to propel the vehicle from the current speed until v_{max} with the constant acceleration a_{pr}. Then, taking into account the minimum SOE allowed in the SC, the lower SOE by energy is defined as:

$$SOE_{low,E}(k) = \left(\frac{E_{pr}(k) - E_{FC}^{pr}(k)\ \eta_{BO}}{\eta_{SC}\ \eta_{BB}\ E_{SC,0}} \right) + SOE_{min}. \tag{19}$$

The condition $SOE(k) \geq SOE_{low,E}(k)$ assures that the vehicle has the required energy for the trip, i.e. the SOE constraint will not be activated. In addition, the constraint associated with the maximum SC current is potentially activated, specially when SOE is low due to that the voltage falls and the current rises noticeably. To avoid that, a lower SOE by current, namely $SOE_{low,I}$, is found so that when $SOE(k) > SOE_{low,I}$, a power flow in the Buck/Boost equal to P_{BB}^{max} produces a current on the SC side lower than I_{BB}^{max}. By using the SC model, this condition leads to:

$$SOE(k) \geq \left(\frac{\eta_{BB}^{-1} P_{BB}^{max}}{I_{BB}^{max}} + R_{SC}\ I_{BB}^{max} \right)^2 \frac{C_{SC}}{2E_{SC,0}}. \tag{20}$$

The right side of this expression is the lower limit by current ($SOE_{low,I}$). Notice that, unlike the Eq. (19), $SOE_{low,I}$ does not depend on k. Finally, the lower SOE limit for the strategy is computed as follows:

$$SOE_{low}(k) = \max\{SOE_{low,E}(k); SOE_{low,I}\}. \tag{21}$$

Higher state of energy

The higher state of energy, namely SOE_{hi}, is computed so that if the current SOE is lower than SOE_{hi}, the SC is able to recover all the energy from the wheels and from the FC during a braking trip from the current speed until it stops. This condition can be expressed as follows:

$$\frac{E_{SC}^{str}(k)}{\eta_{SC}} \geq \left(E_{br}(k) + E_{FC}^{br}(k)\ \eta_{BO} \right)\ \eta_{BB}, \tag{22}$$

where E_{SC}^{str} is the maximum energy that can be stored in the SC from the current state; E_{br} is the energy delivered to the DC-BUS from the regenerative braking; and E_{FC}^{br} is the minimum energy delivered by the FC during this trip. $E_{br}(k)$ can be computed from Eq. (15), with $v_0 = v(k)$ and $v_f = 0$, and using the component efficiencies, it is:

$$E_{br}(k) = -E_{trip}(k)\ \eta_{DF}\ \eta_{EM}. \tag{23}$$

Then, to compute E_{FC}^{br} it is assumed that, from the current state, the FC falls its power up to zero as fast as possible, resulting in:

$$E_{FC}^{br}(k) = \frac{x_{FC}^2(k)}{-\Delta P_{FC}^{min}\ 2}. \tag{24}$$

On the other hand, the energy that can be stored in the SC is computed as:

$$E_{SC}^{str}(k) = (E_{SC,0} - E_{SC}(k)). \tag{25}$$

Now, replacing in (22), solving for E_{SC} and expressing E_{SC} in term of SOE results:

$$SOE(k) \leq 1 - \frac{\left(E_{br}(k) + E_{FC}^{br}(k)\ \eta_{BO} \right)\ \eta_{BB}\ \eta_{SC}}{E_{SC,0}}. \tag{26}$$

The right side of this expression is the higher SOE reference (SOE_{hi}). Fulfilling (26), the SC is able to store the energy from the wheels and from the FC during a braking trip from the current speed until it stops.

3.2 Fuel cell power reference

Once the SOE limits were computed, the current state of propulsion system is classified into one of the three modes, and according to the current mode, the first FC power reference is computed:

$$P_{FC,1}^*(k) = \begin{cases} 0 & \text{if } SOE(k) > SOE_{hi}(k)\ (\textit{Overcharged}) \\ \max\left\{ \frac{P_{CON}^{req}(k)}{\eta_{BO}}; P_{FC}^{opt} \right\} & \text{if } SOE_{low}(k) \leq SOE(k) \leq SOE_{hi}(k)\ (\textit{Charged}) \\ P_{FC}^{max} & \text{if } SOE(k) < SOE_{low}(k)\ (\textit{Discharged}), \end{cases} \tag{27}$$

where P_{FC}^{opt} is the FC power with maximum efficiency. Notice that in the *Overcharged* mode, the FC power reference equal to zero aiming to reduce the SOE, while in case of *Discharged* mode, the FC power reference equal to P_{FC}^{max} aiming to increase the SOE. On the contrary, in case of *Charged* mode, the objective is to remain in this mode, and by setting $P_{CON}^{req}(k)/\eta_{BO}$ as power reference, a tracking of the demanded power is intended. In addition, in this mode, to avoid operating the FC at low efficiency, the FC power reference was limited to a minimum of P_{FC}^{opt}.

Then, a new FC power reference, namely $P_{FC,2}^*$, is computed from $P_{FC,1}^*(k)$ by introducing an upper power limit. Such limit aims to avoid to exceed the maximum power allowed in the Buck/Boost converter, specially during braking situations. According to the power balance in the DC-BUS, the maximum power that FC could deliver without exceeding $P_{BB,max}$ is:

$$P_{FC}^{max,BB}(k) = \frac{P_{CON}^{req}(k) + P_{BB}^{max}}{\eta_{BO}}. \tag{28}$$

Now, the new FC power reference is:

$$P_{FC,2}^*(k) = \min\left\{ P_{FC,1}^*(k); P_{FC}^{max,BB}(k) \right\}. \tag{29}$$

Before computing the control input, the FC reference is bounded according to the maximum and the minimum values, it is:

$$P_{FC}^*(k) = \max\{\min\{P_{FC,2}^*(k); P_{FC}^{max}\}; 0\}. \tag{30}$$

Then, the reference of control input is:

$$\Delta P_{FC}^*(k) = P_{FC}^*(k) - x_{FC}(k). \tag{31}$$

Finally, by using the power rate constraints, the value of control input is obtained:

$$\Delta P_{FC}(k) = \max\left\{ \min\left\{ \Delta P_{FC}^*(k); \Delta P_{FC}^{max} \right\}; \Delta P_{FC}^{min} \right\}. \tag{32}$$

4. SIMULATION RESULTS

The proposed strategy is evaluated by simulation under real driving conditions. The results are compared with those obtained with the ECMS and with the optimal offline solution obtained by using Dynamic Programming.

Table 1. FCHV parameters

Total mass	m	14100	Kg
Frontal area	A_f	8.06	m^2
Drag coefficients	C_x	0.65	-
Rolling coefficient	r_0	0.008	-
	r_1	0.00012	sm^{-1}
Wheel radius	R_{wh}	0.51	m
Differential, ratio	i_{DF}	12.3	-
Differential, Effic.	η_{DF}	0.96	-
EM, Power max.	P_{EM}^{max}	140	kW
EM, Torque max.	T_{EM}^{max}	1380	Nm
EM, Effic.	η_{EM}	0.91	-
FC, Power max.	P_{FC}^{max}	48	kW
FC, Effic. max.	η_{FC}	59% at 20kW	-
FC, Power rise. max.	ΔP_{FC}^{max}	4.8	kW/s
FC, Power fall. max.	ΔP_{FC}^{min}	-4.8	kW/s
Boost, Power max.	P_{BO}^{max}	50	kW
Boost, Effic.	η_{BO}	0.95	-
SC, rated capacity	C_{SC}	702	F
SC, resistance	R_{SC}	0.065	Ω
SC, max. voltage	U_{SC}	325	V
SC, SOE allowed min.	SOE_{min}	0.25	-
SC, SOE allowed max.	SOE_{max}	1	-
Buck/Boost, Power max.	P_{BB}^{max}	100	kW
Buck/Boost, Efficiency	η_{BB}	0.95	-
Buck/Boost, Current max.	I_{BB}^{max}	500	A

Table 2. Properties of the driving cycles

Property	BABC	MBC
Max. speed $[ms^{-1}]$	15.6	11.24
Average speed $[ms^{-1}]$	3.85	4.74
Max acceleration $[ms^{-2}]$	1.54	2.04
Max deceleration $[ms^{-2}]$	-2.16	-2.49
Average acceleration $[ms^{-2}]$	0.41	0.54
Average deceleration $[ms^{-2}]$	-0.42	-0.66

4.1 Case study

The test case chosen corresponds to a hybrid bus used for urban transport. The sizing of FC and SC was addressed following the guidelines reported by Feroldi and Carignano (2016). The parameters of FCHV are listed in Table 1. Regarding the driving conditions, in this work two driving cycles were used. The first one corresponds to buses used for urban transport in the city of Buenos Aires, namely Buenos Aires Bus Cycle (BABC) [1] (Carignano et al. (2016a)), while the second is the standard speed profile Manhattan Bus Cycle (MBC) (Barlow et al. (2009)). Table 2 shows the properties of the driving cycles.

4.2 Adjustment of the strategies

The new strategy presented in this work, EBES, has three adjustable parameters: maximum speed reference v_{max}; acceleration in propulsion trips a_{pr}; and acceleration in braking trips a_{br}. They were adjusted by observing the average values of these magnitudes in the cycle BABC. Accordingly, the parameters were set as follows: $v_{max} = 13\ m/s$, $a_{pr} = 0.8\ m/s^2$ and $a_{br} = 1.3\ m/s^2$. Note that the chosen values a_{pr} and a_{br} are higher (in absolute value) than the averages shown in the table 2. This is because the last ones include idle periods, but for the EBES they are computed without idle periods. With respect to the maximum speed reference chosen, it corresponds to the average of "local" maximum speeds observed in BABC. On the other hand, the ECMS has three adjustable parameters: the equivalents factors s_{chg} and s_{dis}; and the time horizon t^h. The equivalent factors were adjusted following the methodology described in Rodatz et al. (2005), using the cycle BABC, resulting in $s_{chg} = 1.92$ and $s_{dis} = 2.29$. Alternatively, the time horizon was adjusted by simulation, getting the best results with $t^h = 10\ s$. Finally, concerning the optimal strategy, Dynamic Programming was implemented using x_{FC} and SOE as state variables, ΔP_{FC} as control input, and the H_2 consumption as cost function. A vectorized implementation has been adopted according to guidelines from Carignano et al. (2016b).

[1] It was created by ITBA, Instituto Tecnológico de Buenos Aires.

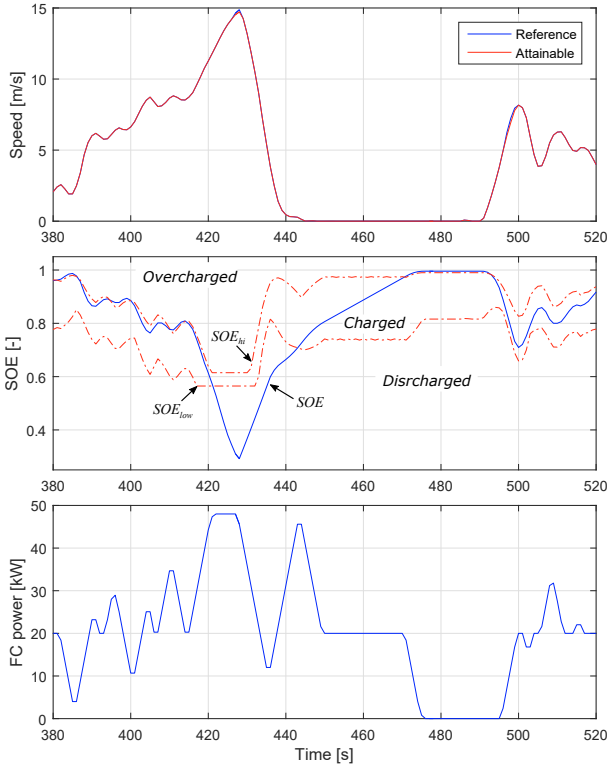

Fig. 3. Segment of simulation using EBES

4.3 Results

Figure 3 shows a segment of simulations where the three modes of the strategy appear. In this figure can be also observed that the speed required was not fulfilled around $t = 430$ and around $t = 495$. Now, the performance obtained with the different strategies are compared. The indicators used for comparison are: H_2 consumption, degree of power compliance and the energy dissipated in the ESS. The degree of power compliance accounts for the fulfillment of the positive power demanded by the Converter in the DC-BUS. It is computed as follows:

$$DoC[\%] = \frac{\sum_{k=1}^{N} P_{CON}^{+}(k)}{\sum_{k=1}^{N} P_{CON}^{req+}(k)} \times 100, \tag{33}$$

where the superscript + means that only positive powers are included in the sum. Then, the energy dissipated in the ESS accounts for the percent of regenerative energy that could not be stored in the ESS because active constraints. It is computed as follows:

Table 3. Performance in BABC

Strategy	H_2 $[Kg/100km]$	DoC [%]	E_{diss} [%]
Novel EBES	5.76	98.1	12.36
ECMS	5.85	97.5	17.18
Optimal strategy	4.99	100	5.83

$$E_{diss}[\%] = \frac{\sum_{k=1}^{N} P_{diss}(k)}{\sum_{k=1}^{N} P_{CON}^{-}(k)} \times 100, \quad (34)$$

where P_{CON}^{-} means that only negative powers are included in the sum. Regarding the H_2 consumption, to make a fair comparison, the difference between the initial and final SOE at the end of the cycle is compensated by adding (or subtracting) an amount of H_2 equivalent to the H_2 consumed. Such compensation was made by using the equivalent factors of the ECMS. Table 3 shows the results obtained in the cycle BABC. As can be observed, a reduction of 1,5% in H_2 consumption is achieved with the present strategy respect to EMCS, while the power compliance is slightly improved. Alternatively, the performance obtained with EBES shows a difference around 13% on fuel economy with respect to optimal solution. These results are consistent with the values of energy dissipated on ESS, in which the optimal strategy presents the minimum percentage and ECMS the maximum percentage.

Now, in order to analyze the robustness of the strategies against driving cycle condition, the strategies were tested in the cycle MBC keeping the parameters adjusted for BABC. Table 4 shows the result obtained.

Table 4. Performance in MBC

Strategy	H_2 $[Kg/100km]$	DoC [%]	E_{diss} [%]
Novel EBES	5.63	99.5	11.2
ECMS	6.37	98.9	26.6
Optimal strategy	4.86	100	3.6

As can be seen, the difference in fuel economy between EBES and ECMS is 12%, while in comparison with the optimal solution, EBES requires 15% more H_2. Again in this case, the correspondence between H_2 consumption and energy dissipated on ESS is evident. These results show another important feature, that the strategy proposed maintain its efficiency performance against variation in driving cycle conditions. It is worth mentioning that the performances of the real time strategies depend strongly on the adjustment of their parameters. In this sense, a reduction on fuel consumption can be achieved in both strategies, but at the expense of a reduction in the DoC.

5. CONCLUSION

In this work a new EMS for a FCHV based on estimation of future energy demand was presented. Results obtained by simulation under real driving conditions show improvements on H_2 consumption compared to ECMS. Secondly, the results presented show that the fuel economy is directly associated with the energy dissipated in the ESS, i.e. the amount of energy that could not be stored in SC because of active constraints. This explains that the strategy ECMS, that basically solves a local optimization problem without forecasts about near future, presents higher values of energy dissipated, and consequently the highest H_2 consumption. On the contrary, the strategy proposed herein prevents active constraint situations by using trip energy estimations, and therefore reduce the energy dissipated in the ESS. Alternatively, the parameters used to adjust the strategy proposed are directly related to the driving profile, which simplified the tuning processes. Regarding the computational effort to compute the control input, the proposed strategy performs simple math and logical operations, which makes it suitable for real-time application.

REFERENCES

Barlow, T., Latham, S., McCrae, I., and Boulter, P. (2009). A reference book of driving cycles for use in the measurement of road vehicle emissions. *TRL Published Project Report*.

Borup, R., Meyers, J., Pivovar, B., Kim, Y.S., Mukundan, R., Garland, N., Myers, D., Wilson, M., Garzon, F., Wood, D., et al. (2007). Scientific aspects of polymer electrolyte fuel cell durability and degradation. *Chemical reviews*, 107(10), 3904–3951.

Carignano, M.G., Adorno, R., Van Dijk, N., Nieberding, N., Nigro, N.M., and Orbaiz, P. (2016a). Assessment of energy management strategies for a hybrid electric bus. In *International Conference on Engineering Optimization*.

Carignano, M.G., Nigro, N.M., and Junco, S. (2016b). HEVs with reconfigurable architecture: a novel design and optimal energy management. In *Integrated Modeling and Analysis in Applied Control and Automation (IMAACA), 2016 I3M*, 59–67.

Feroldi, D., Serra, M., and Riera, J. (2009). Energy management strategies based on efficiency map for fuel cell hybrid vehicles. *Journal of Power Sources*, 190(2), 387–401.

Feroldi, D. and Carignano, M. (2016). Sizing for fuel cell/supercapacitor hybrid vehicles based on stochastic driving cycles. *Applied Energy*, 183, 645–658.

Guzzella, L., Sciarretta, A., et al. (2007). *Vehicle propulsion systems*, volume 1. Springer.

Motapon, S.N., Dessaint, L.A., and Al-Haddad, K. (2014). A comparative study of energy management schemes for a fuel-cell hybrid emergency power system of more-electric aircraft. *IEEE Transactions on Industrial Electronics*, 61(3), 1320–1334.

Pollet, B.G., Staffell, I., and Shang, J.L. (2012). Current status of hybrid, battery and fuel cell electric vehicles: From electrochemistry to market prospects. *Electrochimica Acta*, 84, 235–249.

Rodatz, P., Paganelli, G., Sciarretta, A., and Guzzella, L. (2005). Optimal power management of an experimental fuel cell/supercapacitor-powered hybrid vehicle. *Control Engineering Practice*, 13(1), 41–53.

Strahl, S., Gasamans, N., Llorca, J., and Husar, A. (2014). Experimental analysis of a degraded open-cathode pem fuel cell stack. *International journal of hydrogen energy*, 39(10), 5378–5387.

Sulaiman, N., Hannan, M., Mohamed, A., Majlan, E., and Daud, W.W. (2015). A review on energy management system for fuel cell hybrid electric vehicle: Issues and challenges. *Renewable and Sustainable Energy Reviews*, 52, 802–814.